X-Ray Reflectivity Analysis Incorporated with Genetic Algorithm to Analyze the Y- to X Type Transition in CdA LB Film

Jeong-Woo Choi*, Kyung Sang Cho, Hee Woo Rhee, Won Hong Lee, and Han Sup Lee†

Department of Chemical Engineering, Sogang University, Seoul 121-742, Korea
†Department of Textile Engineering, Inha University, Incheon 402-751, Korea
Received December 4, 1997

The structure and layer distribution of cadmium arachidate Langmuir-Blodgett film were analyzed by the small angle X-ray reflectivity measurements using synchrotron radiation. Y- to X type transition was occurred during the 39th passage of deposition of cadmium arachidate. Based on the measurement of the consumed area of the monolayer, it was determined that about 27.5 layer was deposited. Using the synchrotron X-ray, the reflectivity profile of cadmium arachidate LB film over the wide range of grazing angle was obtained. The X-ray reflectivity profile was analyzed using the recursion formula. By fitting the location and dispersion of the subsidiary maxima between the Bragg peaks of the measured reflectivity profile with that of the calculated reflectivity profile, the average thickness and the distribution of layer thickness were evaluated. The genetic algorithm was adopted to the fitting of reflectivity profile to evaluate the optimum value of the number distribution of layer. Based on the morphology measurement with an atomic force microscopy (AFM), the domain structure and mean roughness of LB films were obtained. The mean roughness value calculated based on the number of layer distribution obtained from the measurement by AFM is consistent with that obtained from X-ray reflectivity analysis.

Introduction

As the fabrication method of angstrom ordered ultra thin organic films, Langmuir-Blodgett (LB) film technique has been used due to the various advantages such as highly ordered packing, controlled orientation and order of molecular array, and film formation at room temperature and pressure.[1] Since the ordered structure of LB films exhibit the optical and electrical characteristics in the molecular level, LB film technique has been applied to the formation of molecular electronic devices.[1-6] However, due to the problems such as defects during the deposition, it is difficult to obtain the desired distribution of films. Especially, for some amphiphiles, it has been observed that transfer ratio (τ=area of monolayer from the subphase/area of substrate) on the upstrokes decreases gradually as the film thickness increases, which indicates the formation of defects. This phenomena has been known as XY-type deposition or a transition deposition from Y- to X-type deposition.[7,8] The mechanisms of the transition deposition have been studied.[7-10] From a morphological point of view, the molecular overturning model[7] and molecular peeling model[8] were proposed. It was proposed that molecules detach during upstrokes and that detached molecules finally return to the film by reattachment or *via* the floating monolayer. This kind of defects makes LB film thickness to be nonhomogeneous. To find the thickness and distribution of XY-type LB film, the measurement and analysis of soft X-ray reflectivity measurement have been performed[9] and optimum number distribution of layer was found using trial and error method. In this study, the structure and the number distribution of layer of XY-type CdA LB film were analyzed using small-angle X-ray reflectivity which has been widely used. From the structural analysis method using recursion formula,[11] many authors have been observed the structure of lipid multilayer LB films.[12,13] But the structure analysis was performed only small number of LB film layer with the unique film layer number (no number layer distribution). In the small number of (<10) unique layer LB film, the subsidiary maxima represent the inner structure of lipid LB film.

In this study, the thickness and distribution of XY-type cadmium arachidate (CdA) LB film was investigated by the small-angle X-ray reflectivity measurement using synchrotron radiation. The analysis method to fit the small subsidiary maxima oscillation profiles between Bragg peaks was proposed. The peak location and oscillation period of the subsidiary maxima between the Bragg peaks were used to evaluate the average number of the deposited layer. Based on the dispersion and decay of oscillating amplitude of subsidiary maxima, the distribution of layers of different thickness was estimated. Genetic algorithm was incorporated into the analysis of the reflectivity profile to find the optimum number distribution of layer of CdA LB film. To evaluate the thickness and distribution obtained by X-ray analysis, morphology observation by an atomic force microscopy (AFM) was also done. The average roughness value and histogram of stacked layer thickness distribution obtained by AFM were well correlated with those evaluated by small-angle X-ray analysis method.

Experimental Details

The measurement of surface pressure-area isotherm and the deposition of LB films were carried out using a rectangular Langmuir trough (Type 611, Nima Tech., England). The deionized ultrapure water (>18MΩ/cm) with 4×10^{-4} M $CdCl_2$ and 5×10^{-5} M $KHCO_3$ was used as a subphase. The pH of the subphase was 6.5 and the temperature was kept at 20 °C. 1 mM arachidic acid solution dissolved in the chloroform was spread on the subphase using 100 μL

micro syringe. Silicon wafer was treated as the surface to be hydrophilic. Since the non-polished side of the silicon substrate may disturb the transfer process during deposition, two silicon wafers were bound to expose only the polished side of the silicon wafer. The substrate was passed through the air-water interface 39 times. The drying time during each stroke was 1,000 sec. The surface pressure and dipping speed were kept to be 15 mN/m and 0.7 mm/min, respectively. The X-ray reflectivity was measured at the Beam Line 3C2, Pohang Accelerator Lab. (PLS) in Korea, using monochromatic synchrotron X-ray radiation (λ=1.608 Å) and the four circle goniometer. Beam Line structure at PLS is described elsewhere.[14] The morphology observation and average roughness measurement was done using a AFM (Autoprobe CP, Park Scientific Instruments, USA). The average thickness was measured with an ellipsometry (Rudolph model 2000, USA).

Results and Discussion

Y- to X-type deposition CdA LB film. Figure 1 shows the decrease of the monolayer area as a function of the dipping cycles during the 39 passages for the deposition of CdA LB film. Initially Y type deposition was observed but, as the number of passages increased, the film deposition became X type. This result represents the transition from Y- to X-type deposition. It was observed that about 27.5 layers of CdA were deposited after the 39th passage. Using the ellipsometry, the average thickness was obtained as 780 Å, which corresponds to the 27.9 layers of CdA LB film based on the 27.95 Å of monolayer CdA LB film.[13] This result is consistent with the average deposited layer obtained by measuring the consumed area of monolayer on the subphase surface.

X-ray reflectivity analysis. The distribution of CdA LB film of different thickness was analyzed by the reflectivity measurement using synchrotron radiation. The reflectivity profiles vs. grazing angle (θ) of CdA LB film deposited 39 times is shown in Figure 2. The cross-sectional size of the incident beam was about 0.5 mm × 1 mm. Since the oscillation of the reflectivity due to the interference of the waves reflected at the air surface and interfaces between

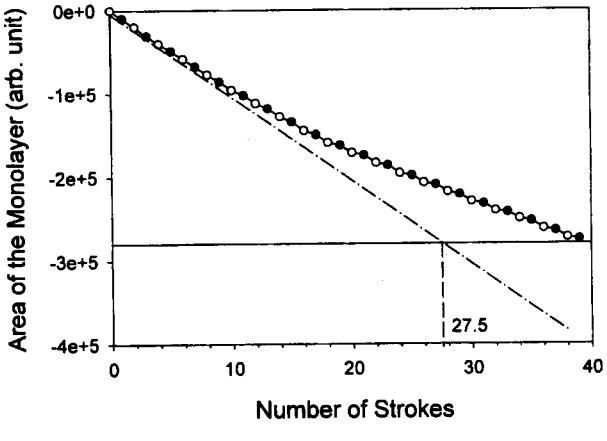

Figure 1. Measured consumption of the floating monolayer of cadmium arachidate after every stroke: ○→●, upstroke; ●→○, downstroke, - · - · -, Y-type deposition.

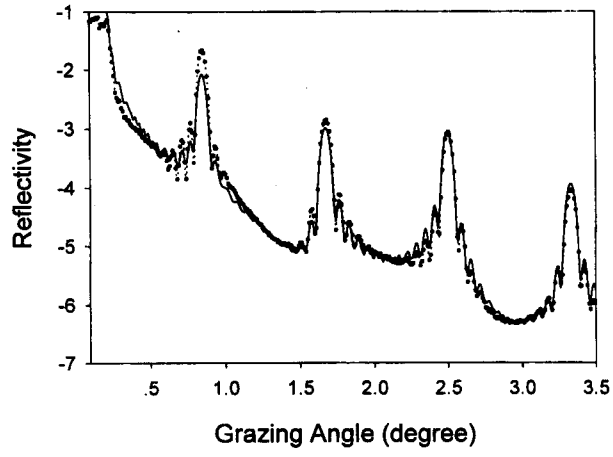

Figure 2. Reflectivity *vs.* θ of cadmium arachidate LB film: ···, measurement; —, calculation.

Table 1. Summary of fit parameters for a cadmium arachidate chain

Layer	Thickness normal to surface (Å)	δ ($\times 10^{-6}$)	k ($\times 10^{-6}$)
Cd	1.2	8.6	0.11
COO	2.1	6.4	0.10
$(CH_2)_{19}$	23.6	3.9	0.05
H	0.8	0.7	0.01

Other parameters
SiO_2 substrate: $\delta = 7.55 \times 10^{-6}$, $k = 0.17 \times 10^{-6}$
Cross sectional area per chain: 18 Å

Where δ and k are the parameters of recursion formula[11]

the layers was observed, the average thickness and the thickness distribution can be calculated by analyzing the oscillation. To get the distribution of CdA LB film having different thickness, the peak profiles of X-ray reflectivity were fitted using structural analysis method.[15] With the electron density profile and optical properties of the LB film,[9] the reflectivity pattern was calculated using the Parrat's recursion formula.[11] The parameters for CdA LB film in recursion formula is listed in Table 1. During the calculation, the uncertainty of the incident angle due to the finite beam size was incorporated in the calculated pattern by convoluting the gaussian function to the reflectivity pattern that was obtained by assuming no uncertainty in the incident angle. The roughness between each stack and air surface and background scattering due to the stray light in the incident beam were also considered by introducing the roughness factor and background as a adjusting parameter. The gradual transition of the electron density at the interface and inside the stack was also incorporated into the calculation by modeling the transitional region as multiple stratified layers of about 3-5 Å thickness. From the angle intervals between the two adjacent Bragg peaks of the reflectivity profile, the d-spacing of bilayer CdA LB film can be accurately obtained. In addition to the major Bragg peaks, there are many small oscillating peaks, which shows the expanded region around first Bragg peaks.

Figure 3(a) shows the calculated X-ray peak profiles around the first Bragg peaks of different layer number of

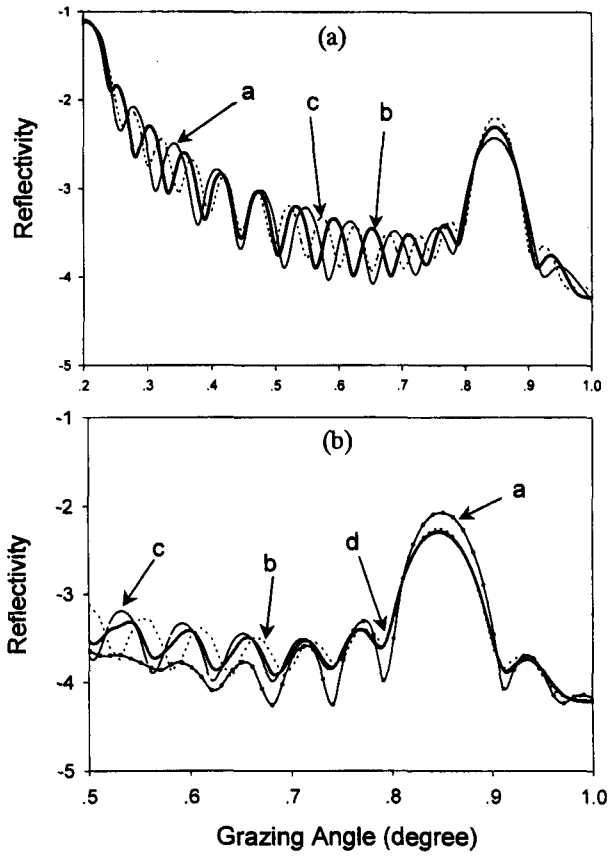

Figure 3. Calculated X-ray reflectivity profile near the 1st Bragg Peak: (a) curve a, 23 layer; curve b, 27 layer, curve c, 31 layer; (b) curve a, measurement; curve b, 27 layer; curve c 29 layer, curve d, 27 layer: 29 layer=7:3.

CdA LB film. As the number of CdA layer increases, the angle intervals between the subsidiary maxima around the Bragg peaks becomes shorten. Based on the calculated peak profiles, the angle interval between these subsidiary peaks can be determined by overall number of stacks in LB layers. Figure 3(b) shows that the average number of stacks was calculated to be about 27-29. The exact distribution of the layers having different number of stacks can not be uniquely determined with X-ray reflectivity measurement. By adjusting the relative amount of two different layers, the position of the subsidiary peaks could be changed. For 70% of 27 layer mixed with 30% of 29 layer (average layer=27.6), the location of the small oscillation peaks is well correlates with the measured value. However, whereas the small oscillation damps out at the angles away from the Bragg angles in the experimental results, the oscillation between Bragg peaks of the calculated profile persists in the case of 70/30 mixture. This results seems to indicate that the actual LB film consists of more than two layers of different thickness. In this case, the calculated X-ray reflectivity profiles is a superposition of oscillation pattern corresponding the various film thickness. Thus, the reflectivity R can be described by

$$R = \sum_{i=0}^{n} w_i R_i \qquad (1)$$

where R_i is the reflectivity of an i-layered film obtained from recursion formula and w_i is the weighting factor. n is the number of the strokes. The number distribution of layers is obtained by best fitting the observed reflectivity profile with w_i as parameters. To find the optimum w_i values, the genetic algorithm was used.

Calculation of optimum distribution function using a genetic algorithm. Genetic algorithm was introduced to find the optimum values of the parameters (w_i) in the calculation of X-ray reflectivity profile. The advantage of the genetic algorithm is the no need of mathematical model or equation during the optimization by making binary code strings corresponds to typical value. Also local minima problems can be avoided by using the population of chromosome. Genetic algorithm is a kind of optimization or search algorithm based on the natural selection and natural generation. It is a stochastic search method based on the principles of three operations (reproduction, crossover and mutation) that is inspired by Darwinism evolution theory; a natural evolution of selection by fitness.[16] It represents the variables in search into a binary code string which is referred to a chromosome. The values of parameters (w_i) are encoded to the binary code strings to be used in the genetic algorithm. A population of chromosome is prepared optionally by random function and their performance are evaluated by actually applying these binary encoded parameters to the objected system. The measurement of performance is a real number which is referred to a fitness value. The fitness function is shown in Eq. 2.

$$Fitness = \frac{K}{\sum_{i=1}^{n} |y_{set} - y_i| + (y_{set} - y_i)^2} \qquad (2)$$

where K is constant and y_{set}, y_i are the set point value and measured value in the genetic algorithm, respectively. After the evaluation of each fitness value, all the chromosomes are combined each other through genetic operators to reproduce a new set of chromosome to be evaluated. Genetic operators are prepared as the following variations; reproduction, crossover and mutation. In the reproduction, population of binary code strings are reproduced. Each individual's

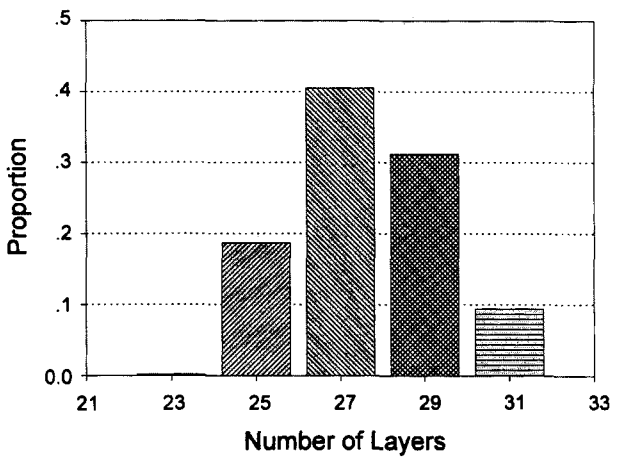

Figure 4. Number distribution of layer after the 39th stroke measured using X-ray reflectivity.

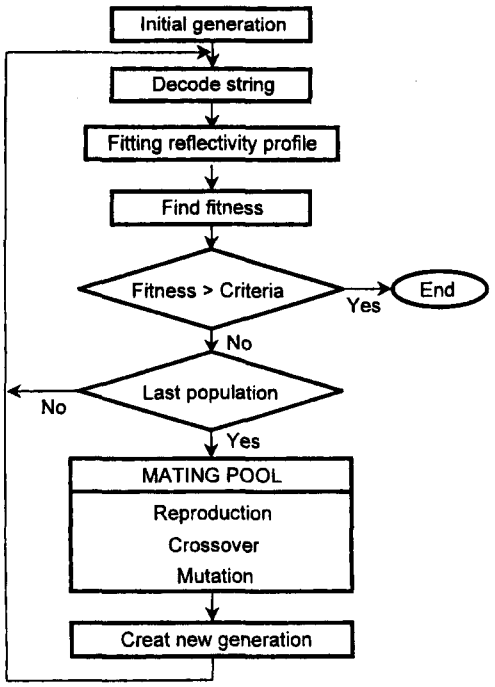

Figure 5. Overall procedure of the optimum number distribution of layer.

probability of being reproduced is proportional to the string's fitness. The crossover operator simulates the recombination of genetic elements made possibly by sexual modes of reproduction. Crossover begins with the selection of a random integer larger than zero and less than the string length, defining thereby a crossover point. Two strings are mated by joining the prefix of one string with the suffix of the other string relative to the crossover point. With any sparse search through a large parameter space there is a danger of converging on a solution that is only locally rather than globally optimal. To avoid such traps, mutations are introduced after crossover. Each binary digit has some small probability of being reversed during the genetic recombination.

The overall process of optimum number layer distribution using genetic algorithm is shown in Figure 5. Maximum and average fitness values were increased as the generation number increased as shown in Figure 6. Optimum w_i values can be chosen at the generation having the highest average fitness value. Figure 2 shows that the experimental reflectivity profile is very closely simulated with the calculated reflectivity profile obtained with the layer distribution portion of 23 : 25 : 27 : 29 : 31 layers=0.02 : 0.14 : 0.43 : 0.34 : 0.07 which were obtained using genetic algorithm. Not only the location and relative intensity of the Bragg peaks but also the location of the subsidiary peak are well predicted by the calculation. It is also noted that by introducing many layers of different thickness maintaining the constant average thickness, the damping of the subsidiary peak was successfully predicted and the number of layer distribution could be obtained. The proportion of the layers having different thickness obtained with the proposed analysis is shown in Figure 4.

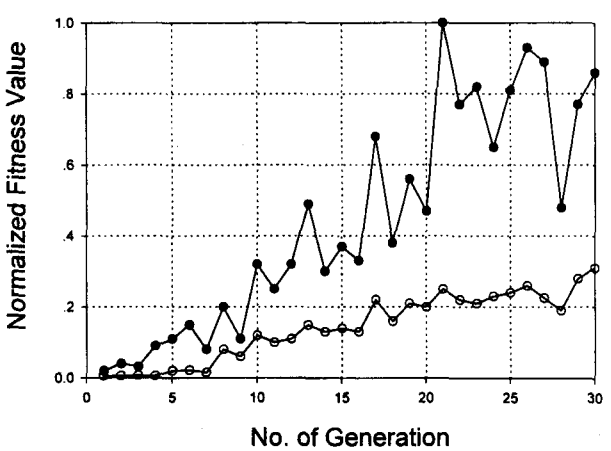

Figure 6. Fitness value of individual generation in simulation: —○— average fitness; —●— maximum fitness.

Mean roughness measurement by AFM. AFM image of the CdA LB film was shown in Figure 7(a). Domain structure was observed in the 5 mm × 5 mm scale. The histogram of the thickness distribution of the inside of the rec-

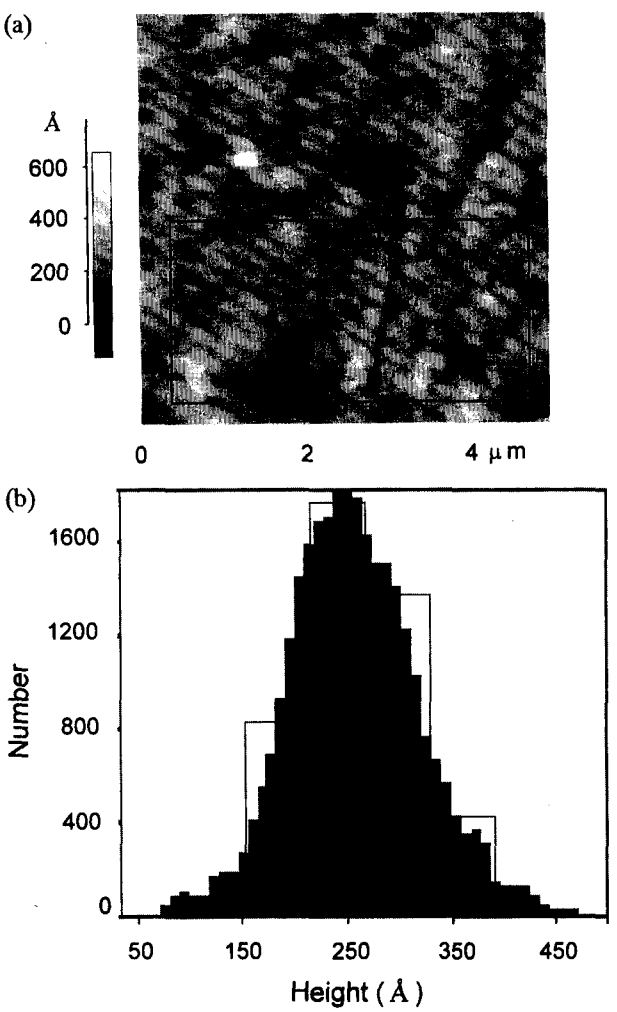

Figure 7. AFM image of cadmium arachidate LB film: (a) 5 μm × 5 μm scale image; (b) height distribution portion of the inside of the rectangle in (a). The superposed histograms are the thickness distribution in Figure 5.

tangle in Figure 7(a) was shown in Figure 7(b). The distribution of layers with different thickness is analogous with that obtained by the X-ray measurement. The average roughness of LB film, 49.6 Å, calculated using the layer distribution in Figure 4 was well consistent with the mean roughness value (49.8 Å) measured by AFM.

Acknowledgment. This work was supported by the Research Fund on the Optical Technology Project (F-15, 1996) of the Korea Ministry of Science and Technology. The X-ray experiments at PLS, Korea, were supported by MOST and POSCO, Korea.

References

1. Ulman, A. *An Introduction to Ultrathin Films*; Academic Press: San Diego, CA, 1991.
2. Choi, J. W.; Jung, G. Y.; Oh, S. Y.; Lee, W. H.; Shin, D. M. *Thin Solid Films* **1996**, *284/285*, 876.
3. Choi, J. W.; Kim, M. J.; Jung, S. W.; Oh, S. Y.; Lee, W. H. *Shin, D. M. Mol. Cryst. Liq. Cryst.* **1996**, *280*, 367.
4. Choi, J. W.; Bae, J. Y.; Min, J.; Cho, K. S.; Lee, W. H. *Sensors and Materials* **1996**, *8(8)*, 493.
5. Choi, J. W.; Kim, M. J.; Jung, S. W.; Oh, S. Y.; Lee, W. H. *Shin, D. M. Mol. Cryst. Liq. Cryst.* **1997**, *294*, 217.
6. Choi, J. W.; Min, J.; Jung, J. W.; Rhee, H. W.; Lee, W. H. *Mol. Cryst. Liq. Cryst.* **1997**, *295*, 153.
7. Honig, E. P. *J. Collid Interface Sci.* **1973**, *43*, 66.
8. Peng, J. B.; Ketterson, J. B.; Dutta, P. *Langmuir* **1988**, *4*, 1198.
9. Momose, A.; Hirai, Y.; Waki, I.; Imazakei, S.; Tomioka, Y.; Hayakawa, K.; Naito, M. *Thin Solid Films* **1989**, *178*, 519.
10. Momose, A.; Hirai, Y. *Thin Solid Films* **1991**, *204*, 175.
11. Parrat, L. G. *Phys. Rev.* **1954**, *95*, 359.
12. Pomerantz, M.; Segmuller, A. *Thin Solid Films* **1980**, *68*, 33.
13. Jark, W.; Comelli, G.; Russell, T. P.; Stohr, J. *Thin Solid Films* **1989**, *170*, 309.
14. Park, B. J.; Rah, S. Y.; Park, Y. J.; Lee, K. B. *Rev. Sci. Instrum.* **1995**, *66(2)*, 1722.
15. Segmuller, S. *Thin Solid Films* **1973**, *18*, 287.
16. Hwang H. S.; Woo, K. B. *J. of Fuzzy Logic and Intelligent System* **1989**, *2(3)*, 40.

Structures and Spectroscopic Properties of OC_nO (n=2-6): Density Functional Theory Study

Kyung-Hwan Kim, Bosoon Lee, and Sungyul Lee*

Department of Chemistry, Kyunghee University, Kyungki-do 449-701, Korea
Received December 16, 1997

Density functional theory calculations are reported for the carbon clusters bonded with two oxygen atoms OC_nO (n=2-6). The structures, vibrational frequencies and dipole moments are computed by BLYP theory with the 6-311G* basis set. Good agreement is obtained between the computed and experimentally observed properties. The ground states of these molecules are shown to be linear. Cyclic structures with higher energy are also predicted.

Introduction

Carbon clusters with polycumulated double bonds of general structure of XC_nY (X, $Y=H_2$, O, S) received considerable attention recently due to the unusual spectroscopic properties and high reactivity. Some of these molecules are known to be very quasilinear.[1] For example, the frequency of the lowest bending mode of the linear molecule OC_3O is only 18 cm^{-1}.[2] The alternation of the electronic multiplicity (singlet for odd n and triplet for even n) and other properties is also characteristic of these molecules. These molecules are not inherently unstable, and the difficulty of preparing them in laboratory is only due to their unusual reactivity. Quantum chemical treatment of these molecules were mostly limited to semiempirical or Hartree-Fock level of methods, due to the large size of the molecules. Interstellar detection of carbon clusters also seems to give these molecules astrophysical importance.

Considering the spectroscopic and astrophysical importance of these molecules, we report in the present work the theoretical calculations by employing the density functional theory,[3,4] which proved[5-9] to give surprisingly accurate spectroscopic properties of medium-sized carbon clusters with much less computational efforts than other correlated *ab initio* methods. We report the spectroscopic properties of the carbon suboxides OC_nO (n=2-6). We employ the BLYP/6-311G* density functional theory. We find that the ground states of these molecules are linear. The computed spectroscopic properties agree well with experimental observations. Predictions are also made for several cyclic

*Corresponding author